# New Directions in HFSS for Designing Microwave Devices

Developed by Ansoft in 1990, the High Frequency Structure Simulator (HFSS) has become the simulator of choice for the electromagnetics design of complex three-dimensional microwave devices. HFSS has been used to design thousands of microwave devices more quickly and reliably than is possible with prototypes alone. This broad use has generated considerable user feedback and customer requests for the software to address new simulation capabilities and directions. Two of the most requested features for Ansoft HFSS are the ability to model the resonance and quality factor of microwave cavities as well as a more broadband fast sweep capability. Another requested feature is the ability to model active devices and phased-array antennas through fields linked by values at two different boundaries. Development of higher accuracy mesh truncation procedures for modeling radiation from antennas, more powerful geometry modeling using precise solids and faster, more complete graphics tools for postprocessing also have been requested.

Version 6 sets a new direction for HFSS in these high impact areas. A new graphical user interface streamlines model creation, simulation and postprocessing. Adaptive Lanczos-Pade sweep (ALPS), a new fast frequency sweep technology, provides a more broadband and reliable fast sweep capability than was available in earlier versions. The ALPS fast sweep capability coupled with a new field calculator allows microwave cavity resonances and quality factors to be determined precisely. The linked boundary condition (LBC), which allows active devices and periodic structures to be modeled, has been added and open boundaries can be modeled more accurately by perfectly matched layers (PML) that mimic free space to a remarkable degree. In addition, the software's geometry entry and postprocessing capabilities have been completely revamped to allow users greater flexibility and freedom in entering geometry and displaying results.

This article highlights two application areas that can be solved for the first time using Ansoft HFSS version 6. The new ALPS fast frequency sweep algorithm and the new field calculator can be used to compute closed-cavity resonant frequencies and quality factors, respectively. Also, large phased-array antennas can be simulated using the simulator's new PML and LBC features.

## Resonance Analysis of Closed Cavities

Resonant microwave devices such as oscillators or filters are often modeled in textbooks as closed cavities. Such mathematical models provide important information for the design of real microwave hardware and allow basic parameters such as resonance frequencies and quality factors to be determined.

Since the excitation should not influence the field in the cavity at resonance, the cavity can be excited by a small, arbitrarily shaped hole on the cavity's surface. The maximal size of the hole must not exceed one-fifth the maximal size of the cavity. Although the shape and location of this hole are arbitrary, at least one component of the field pattern of the exciting port must coincide with one component of the field pattern of the cavity mode. It is customary to choose a circular hole. The smaller the hole, the more accurate the solution. However, a finer mesh is required to model the problem accurately. This hole is treated as a port in the simulator.

An adaptive mesh solution is performed followed by a fast frequency sweep. The fast frequency sweep procedure in HFSS was introduced in 1994 as a way to compute the frequency response of high frequency devices over a limited bandwidth. The original proce-

Istvan Bardi and Zoltan Cendes
*Ansoft Corp.*
*Pittsburgh, PA*

dure was based on asymptotic waveform evaluation (AWE), which provides an efficient mechanism to compute a reduced-order model of microwave devices. The new method searches for the dominant poles and zeros of the network transfer function. (Note that this algorithm computes the fundamental device behavior as opposed to more recent fast sweep procedures in other software that are used as shortcuts and merely

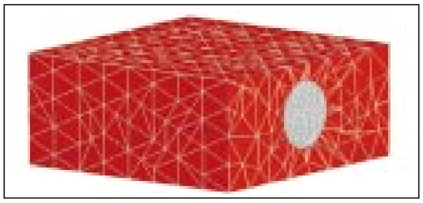

*Fig. 1 A rectangular cavity.*

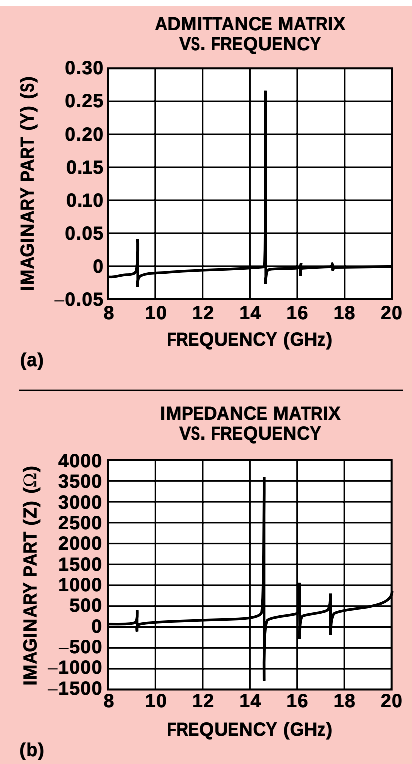


*Fig. 2 The cavity's (a) admittance vs. frequency and (b) impedance vs. frequency.*

fill in discrete sweep values with rational polynomial interpolation.) AWE is based on a power method and excels at locating the frequency response near the specified frequency. The new fast sweep algorithm is based on the Lanczos algorithm and provides a more broadband response. This ALPS procedure is able to locate all resonances in a wide frequency range, identifying the less dominant resonances and, hence, detecting subtleties in the frequency response more easily. ALPS includes port dispersion to determine input power level vs. frequency and out-of-band rolloff more accurately.

Resonant cavities are almost-closed structures, hence, only cavity modes can exist. This fact is reflected in the frequency response of the S parameters. The new ALPS fast frequency sweep procedure is very economical. Usually, the entire fast frequency sweep broadband response is computed in less than 30 percent additional time than is required by a single frequency solution. The total solution time depends on the desired accuracy and the width of the specified frequency range. As many as 1000 division points can be selected without unduly increasing the solution time. Thus, sharp changes can be localized in the frequency response.

A vacuum-filled rectangular box has been investigated with the wall losses taken into account to determine the first four lowest order resonance frequencies and unloaded quality factors. In general, there is no restriction on cavity shape. However, a rectangular cavity has been used here in order to compare with analytical results. The geometry of this cavity is shown in ***Figure 1***. A small central circular hole of diameter D is defined on the surface y = 22.86 mm as an iris. This iris coincides with the port for computing the circuit parameters. The lowest cutoff frequency of a circular waveguide is the $TE_{11}$ mode

$$f_{cutoff} = \frac{0.588c}{D} \qquad (1)$$

where

c = speed of light in a vacuum

In this equation, $f_{cutoff}$ = 29.4 GHz (D = 6 mm) and the applied frequency range is 8 to 18 GHz (below the lowest cutoff).

The admittance and impedance frequency responses are shown in ***Figure 2***. The zeros of the imaginary part of both the admittance and impedance mark the resonance frequencies; their agreement with one another can be used to determine whether or not the finite element mesh is fine enough.

The unloaded quality factor of the resonator is calculated from the magnetic field using

$$Q_u = \frac{\int_\Omega |H|^2 d\Omega}{\frac{s}{2}\oint_\Gamma |n \times H|^2 d\Gamma + tg\delta \int_\Omega |H|^2 d\Omega} \qquad (2)$$

where

s = skin depth of the cavity wall
$tg\delta$ = electric loss tangent of the dielectric inside the resonator, if any

The unloaded quality factor is computed using Equation 2 and the new field calculator in HFSS.

The upgraded field calculator allows complex arithmetic and trigonometric functions, computation of tangents to curved lines and normals to any curved surface. For example, it is now possible to plot the phase of induced current on a curved or planar surface. Evaluating the unloaded quality factor is simple using this new field calculator. Any complicated object can be constructed in the preprocessor using Boolean operations, and the object can be called by its name to perform the volume and/or surface integrals required in Equation 2. These integrals are solved with arbitrary user-defined integrands. (This procedure also is true for the case of normal or tangential vectors to a surface.)

***Table 1*** lists the analytical and simulated values of the resonance frequen-

## TABLE I

**ANALYTICAL/SIMULATED VALUES OF RESONANCE FREQUENCIES/UNLOADED QUALITY FACTORS**

| Mode Indices | $f_{anal}$ (GHz) | $f_{simulated}$ (GHz) | Error (%) | $Q_{anal}$ | $Q_{simulated}$ | Error (%) |
|---|---|---|---|---|---|---|
| TE110 | 9.2796 | 9.2713 | 0.09 | 7816 | 8255 | 5.6 |
| TE210 | 14.6724 | 14.6469 | 0.17 | 9817 | 10,204 | 3.9 |
| TE101 | 16.1563 | 16.1428 | 0.08 | 8703 | 9306 | 6.9 |
| TE111 | 17.4379 | 17.4228 | 0.09 | 7358 | 7864 | 6.8 |

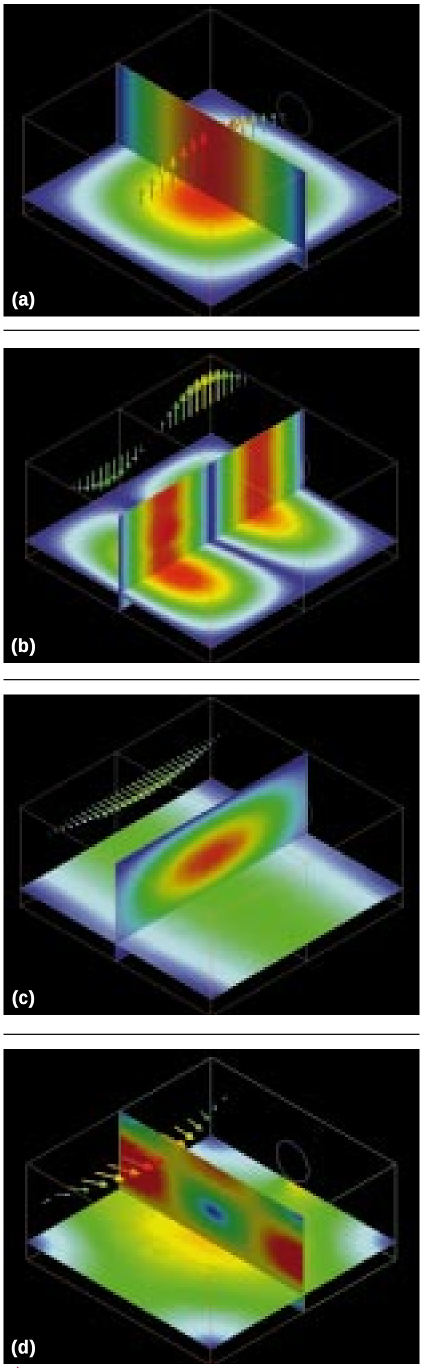


▲ *Fig. 3 The electric field plots for the four resonant modes.*

cies and quality factors for the cavity. ***Figure 3*** shows electric field plots in different planes for the four resonant modes. HFSS version 6 yields the correct resonance frequencies even in the case of multiple resonances. (All resonance frequencies were predicted within 0.17 percent of the analytical values and quality factors were within 6.9 percent.) Note that the analytical solution for quality factor is based on the assumption of a lossless cavity. The simulated results based (more appropriately) on loss cavity fields are believed to be more accurate.

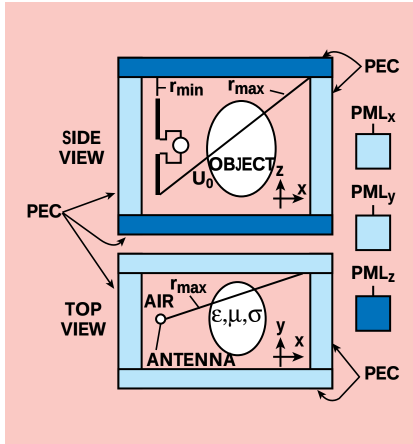


▲ *Fig. 4 A radiation problem bounded by PMLs.*

In the case of degenerate modes that have the same resonant frequency, the field pattern and, therefore, the unloaded quality factor may be difficult to extract due to overlapping of the different field patterns. These problems were avoided in this case since only the TE modes were excited.

## PMLs IN THE HFSS ENVIRONMENT

PMLs have become the focus of much attention recently in the analysis of high frequency fields. Originally proposed by Berenger for the finite-difference time domain method, PMLs have been successfully extended for use with the finite element method. Tests indicate that PMLs are significantly more accurate than conventional absorbing boundary conditions (ABC) for modeling radiation from antennas and scatterers. Version 6 allows PMLs to be used for the first time in HFSS.

The basic concept behind PMLs is to create a fictitious material that fully absorbs the electromagnetic field impinging on it. This material requires both the permittivity and permeability to be complex anisotropic. Ansoft HFSS version 6 has the capability to model both complex tensor permittivity and complex tensor permeability.

### Embedded PMLs

The traditional procedure for analyzing a radiating structure in HFSS is to embed the radiator within an air-filled box. The outermost surface of this box is assigned a radiation boundary condition that utilizes a second-order local ABC. A similar procedure is used with PMLs: The radiator is placed inside an air box. However, instead of placing a single ABC on the outside of the box, several layers of specialized materials are added to absorb the outgoing waves. These PMLs are biaxial anisotropic with special complex material characteristics. A schematic arrangement of a radiation problem bounded by PMLs is shown in ***Figure 4***.

To ensure that there is no reflection at the PML/air interface, the biaxial diagonal material tensors for x-, y- and z-directed PMLs are of the form

$$\frac{[\varepsilon]}{\varepsilon_0} = \left\langle \frac{1}{C} \quad C \quad C \right\rangle; \frac{[\mu]}{\mu_0} = \left\langle \frac{1}{C} \quad C \quad C \right\rangle \tag{3}$$

$$\frac{[\varepsilon]}{\varepsilon_0} = \left\langle C \quad \frac{1}{C} \quad C \right\rangle; \frac{[\mu]}{\mu_0} = \left\langle C \quad \frac{1}{C} \quad C \right\rangle \tag{4}$$

$$\frac{[\varepsilon]}{\varepsilon_0} = \left\langle C \quad C \quad \frac{1}{C} \right\rangle; \frac{[\mu]}{\mu_0} = \left\langle C \quad C \quad \frac{1}{C} \right\rangle \tag{5}$$

where

$C = a - jb$

The tensors in Equation 3 characterize an x-directed PML corresponding to a PML wall in the y-z plane. This x-directed layer is designated $PML_x$. Similarly, Equations 4 and 5 provide tensors for $PML_y$ and $PML_z$, respectively.

PMLs of different directions must be joined in order to construct a box with PML walls. The incident and reflected waves must pass through the PML at least twice for good absorption. A solution is to overlap the layers at the corners as shown.

The next step in embedding a problem in PMLs is to specify boundary conditions on the outer surface of the box. The simplest way is to bind the box either with perfect electric conductors (PEC) or perfect magnetic conductors. PECs are preferred since they reduce the problem size.

### Setting PML Parameters

Setting the proper value of the complex parameter C ensures that the electromagnetic field decays strongly in the PMLs. Back reflec-

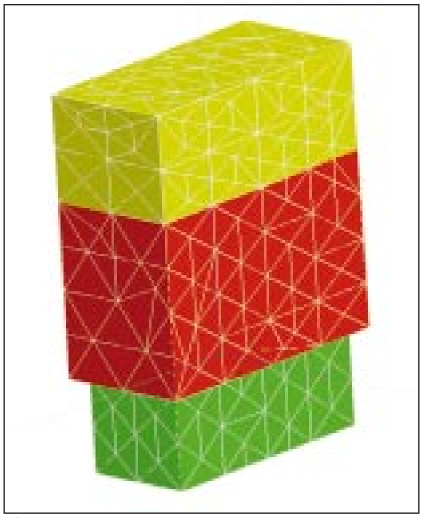

*Fig. 5 An example of a phased-array antenna representation.*

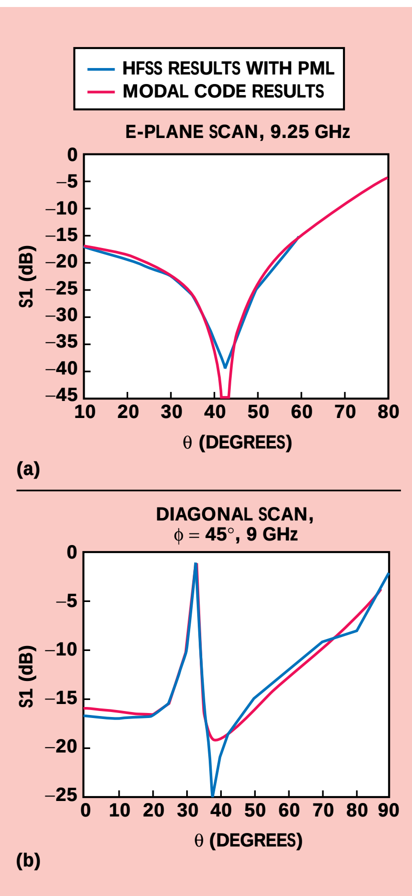


*Fig. 6 S parameters vs. scan angle for the rectangular aperture antenna array.*

tions from the bounding PECs then are kept below a prescribed bound. The number of layers required for the PML region is

$$n = \frac{D_{max} \ln \rho}{D_{min} \ln d} \qquad (6)$$

where

$$D_{min} = \frac{1}{\frac{1}{r_{min}} + \frac{\omega_{max}}{c}}$$

$$D_{max} = \frac{1}{\frac{1}{r_{max}} + \frac{\omega_{min}}{c}}$$

and

$r_{min}$ = minimal distance between the radiating object and PML interface

$r_{max}$ = maximal distance between the radiating object and PML interface

$\omega_{min}$ = minimum angular frequency

$\omega_{max}$ = maximum angular frequency

$\rho$ = maximum back reflection (usually $\rho \leq 10^{-4}$)

d = maximum decay possible in the element

The maximum decay for Ansoft HFSS is

$$d = 3 \bullet 10^{-3} \qquad (7)$$

Knowing the geometry, frequency, ρ and d, the number of layers required for the PML parameter can be calucated using Equation 6. Given n, the value of the PML parameter can be calculated as

$$\begin{aligned} a &= b \\ &= \frac{-D_{min} \ln d}{2h} \\ &= \frac{-D_{max} \ln \rho}{2nh} \end{aligned} \qquad (8)$$

where

h = thickness of an individiual PML

PMLs can be located as close as possible to the radiating objects. However, a consequence of a close setting is that the ratio $D_{max}/D_{min}$ increases so that the number of layers required also increases.

## LBCs IN HFSS

Another new direction in Ansoft HFSS version 6 is the introduction of LBCs, which enable a new class of problems, including active devices, to be modeled by specifying a relationship in the fields between two or more boundaries. LBCs save computer time and memory in modeling long, uniform structures and periodic structures by allowing the user to model only a segment of the structure. The fields at the ends of the structure then are linked by LBCs.

To model a periodic structure, the user defines a master boundary and a slave boundary. By choosing a master boundary and corresponding slave boundary of equal size and shape, the user may specify that the solution on those two boundaries be related through a phase ϕ such that

$$E(slave) = e^{j} E(master) \qquad (9)$$

A proprietary algorithm is used to ensure that the meshes formed on the master and slave boundaries are identical throughout the adaptive mesh generation process.

The new boundary manager is notable for the ease with which users can choose and assign boundaries. As the boundary type is chosen for any boundary, the user is prompted for the required information. For example, choosing an impedance boundary prompts the user for the appropriate resistance and reactance. Choosing master/slave boundary pairs prompts the user for the phase factor between the boundaries. Boundary manager graphics functions — including zoom, pan or rotate — and the ability to hide or show selected parts of the model aid the user in boundary assignment.

## PHASED-ARRAY ANTENNA SIMULATION

An example of a phased-array antenna, as shown in ***Figure 5***, illustrates the use of LBCs in phased-array antenna applications. The antenna comprises a rectangular array of rectangular apertures in a conducting ground plane, each fed from below via a waveguide. The user constructs a model using a unit cell of the antenna array with the modeler. This unit cell is appropriate for an infinite array of rectangular waveguides, 0.4" × 0.9", terminated in a metallic ground plane. The unit cell — and, hence, the array lattice — is 0.5" × 1.0", the waveguide length is 0.35" and the unit cell length is 0.6". In this case, a rectangular unit cell is appropriate; more complicated symmetries can be modeled by changing the shape of the unit cell. The open boundary for this problem has been modeled using PMLs. The PML parameters were

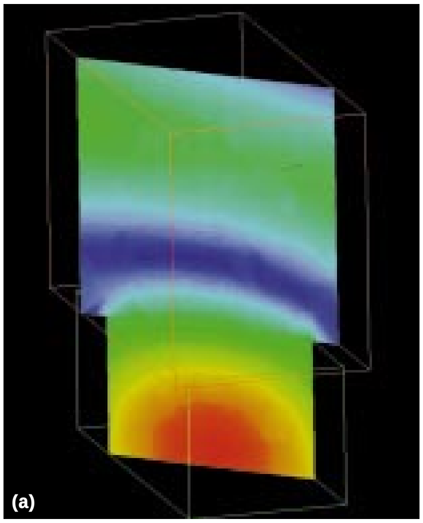

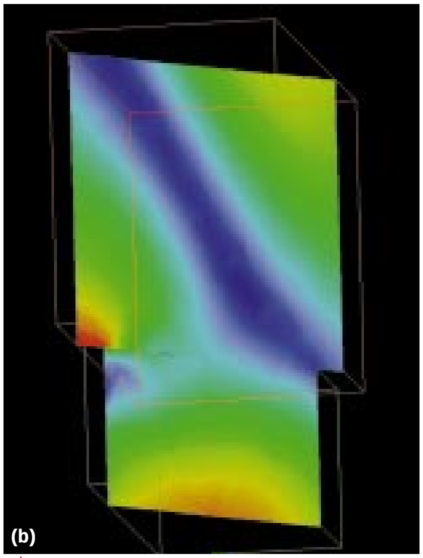

Fig. 7 The E-field pattern at $\phi = 45°$ and $\theta$ = (a) 10° and (b) 70°.

calculated using Equations 6 through 8. Different scan angles were set by changing the phase relationship in the LBC boundaries. The user then is able to calculate reflection loss and scan blindness for any scan angle.

***Figure 6*** shows a plot of S parameters vs. scan angle $\theta$ for the array of rectangular aperture antennas at 9.25 GHz. (The scan is in the antenna's E plane.) $\theta$ is measured from the z-axis down, and the aperture is in the x-y plane. The red line represents results obtained using an independent modal code, and the blue line represents the HFSS results. The HFSS results show good agreement with the modal code results over the entire range of scan angles. Results for the same geometry at 9 GHz for a diagonal plane sweep at $\phi = 45°$ from the E plane are also shown. Again, the HFSS and modal code results are in agreement over the entire range of scan angles. ***Figure 7*** shows the E-field pattern of diagonal scan of $\phi$ = 45° and f = 9 GHz at $\theta$ = 10° and 70°.

## CONCLUSION

Ansoft HFSS version 6 sets a new direction in electromagnetics electronic design automation (EDA). ALPS-based fast frequency sweep technology provides new resonance capability while LBCs and PLMs allow periodic structures and phased-array antennas to be modeled more accurately. These new directions and the new, more powerful user interface make HFSS version 6 an even more versatile electromagnetics EDA tool for microwave engineers.

## ACKNOWLEDGMENT

The authors would like to extend special thanks to John Hadden and Raytheon Systems Co., El Segundo, CA, for providing the modal code phased-array simulation results. ■

## References


1. J.P. Berenger, "A Perfectly Matched Layer for the Absorption of Electromagnetic Waves," *Journal of Computational Physics*, No. 114, 1994, pp. 185–200.
2. Jo-Yu Wu, David M. Kingsland, Jin-Fa Lee and Robert Lee, "A Comparison of Anisotropic PML to Berenger's PML and Its Application to the Finite-element Method for EM Scattering," *IEEE Transactions on Antennas and Propagation*, Vol. 45, No. 1, 1995, pp. 40–50.
3. I. Bardi and Zs. Badics, "Solution of Team Workshop Problem 18 by Maxwell Eminence," presented at the TEAM Workshop meeting held in Rio de Janiero, Brazil, November 7, 1997.
4. X. Yuan and Z. Cendes, "A Fast Method for Computing the Spectral Response of Microwave Devices over a Broad Bandwidth," *Proceedings of the APS/URSI Symposium*, Ann Arbor, MI, June 1993, p. 196.
5. I. Bardi, O. Bíró, K. Preis, W. Renhart and K.R. Richter, "Parameter Estimation for PMLs Used with 3-D Finite Element Codes," submitted for publication to *IEEE Transactions on Magnetics.*
6. E. Brookner, "Major Advances in Phased Arrays: Part I," *Microwave Journal*, Vol. 40, No. 5, May 1997, pp. 288–294.


**Istvan Bardi** *received his Dipl Ing degree in electrical engineering and his Dr Techn degree from the Technical University of Budapest, Hungary, in 1970 and 1983, respectively. In addition, he received the degree of Candidate of Technical Sciences (on the subject of electromagnetic computations) from the Hungarian Academy of Sciences in 1982. From 1970 to 1990, Bardi was with the department of electromagnetic theory at the Technical University of Budapest as an associate professor. He then spent six years with Graz University of Technology, Austria as a guest professor. In 1997, Bardi joined Ansoft Corp., Pittsburgh, PA, where he is currently a senior development engineer. His research deals mainly with numerical methods of electromagnetic field computations, mostly in the fields of microwave applications.*

**Zoltan J. Cendes** *received his doctorate and master's degrees in electrical engineering from McGill University. He is the founder and chief technology officer of Ansoft Corp., Pittsburgh, PA, where he is the technical leader of research and development. In this role, Cendes is responsible for developing the theory behind the HFSS. He is also a professor of electrical and computer engineering at Carnegie Mellon University, Pittsburgh. Cendes served as associate professor of electrical engineering at McGill University, Montreal, Quebec, Canada. His previous experience includes six years with the General Electric Corp.*

# 射 频 和 天 线 设 计 培 训 课 程 推 荐

易迪拓培训(www.edatop.com)由数名来自于研发第一线的资深工程师发起成立，致力并专注于微波、射频、天线设计研发人才的培养；我们于 2006 年整合合并微波 EDA 网(www.mweda.com)，现已发展成为国内最大的微波射频和天线设计人才培养基地，成功推出多套微波射频以及天线设计经典培训课程和 ADS、HFSS 等专业软件使用培训课程，广受客户好评；并先后与人民邮电出版社、电子工业出版社合作出版了多本专业图书，帮助数万名工程师提升了专业技术能力。客户遍布中兴通讯、研通高频、埃威航电、国人通信等多家国内知名公司，以及台湾工业技术研究院、永业科技、全一电子等多家台湾地区企业。

易迪拓培训课程列表：http://www.edatop.com/peixun/rfe/129.html


## 射频工程师养成培训课程套装

该套装精选了射频专业基础培训课程、射频仿真设计培训课程和射频电路测量培训课程三个类别共 30 门视频培训课程和 3 本图书教材；旨在引领学员全面学习一个射频工程师需要熟悉、理解和掌握的专业知识和研发设计能力。通过套装的学习，能够让学员完全达到和胜任一个合格的射频工程师的要求…

课程网址：http://www.edatop.com/peixun/rfe/110.html

## ADS 学习培训课程套装

该套装是迄今国内最全面、最权威的 ADS 培训教程，共包含 10 门 ADS 学习培训课程。课程是由具有多年 ADS 使用经验的微波射频与通信系统设计领域资深专家讲解，并多结合设计实例，由浅入深、详细而又全面地讲解了 ADS 在微波射频电路设计、通信系统设计和电磁仿真设计方面的内容。能让您在最短的时间内学会使用 ADS，迅速提升个人技术能力，把 ADS 真正应用到实际研发工作中去，成为 ADS 设计专家...

课程网址： http://www.edatop.com/peixun/ads/13.html

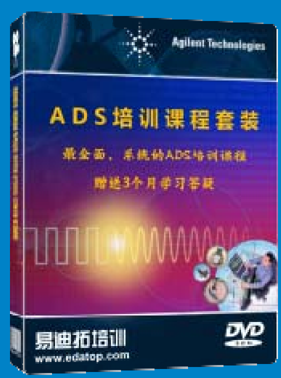



## HFSS 学习培训课程套装

该套课程套装包含了本站全部 HFSS 培训课程，是迄今国内最全面、最专业的 HFSS 培训教程套装，可以帮助您从零开始，全面深入学习 HFSS 的各项功能和在多个方面的工程应用。购买套装，更可超值赠送 3 个月免费学习答疑，随时解答您学习过程中遇到的棘手问题，让您的 HFSS 学习更加轻松顺畅…

课程网址：http://www.edatop.com/peixun/hfss/11.html

## CST 学习培训课程套装

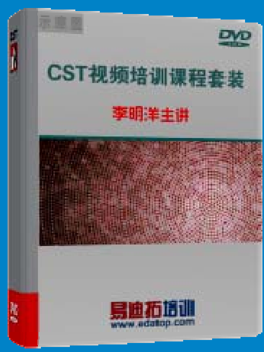


该培训套装由易迪拓培训联合微波 EDA 网共同推出，是最全面、系统、专业的 CST 微波工作室培训课程套装，所有课程都由经验丰富的专家授课，视频教学，可以帮助您从零开始，全面系统地学习 CST 微波工作的各项功能及其在微波射频、天线设计等领域的设计应用。且购买该套装，还可超值赠送 3 个月免费学习答疑…

课程网址：http://www.edatop.com/peixun/cst/24.html

---


## HFSS 天线设计培训课程套装

套装包含 6 门视频课程和 1 本图书，课程从基础讲起，内容由浅入深，理论介绍和实际操作讲解相结合，全面系统的讲解了 HFSS 天线设计的全过程。是国内最全面、最专业的 HFSS 天线设计课程，可以帮助您快速学习掌握如何使用 HFSS 设计天线，让天线设计不再难…

课程网址：http://www.edatop.com/peixun/hfss/122.html

---

## 13.56MHz NFC/RFID 线圈天线设计培训课程套装


套装包含 4 门视频培训课程，培训将 13.56MHz 线圈天线设计原理和仿真设计实践相结合，全面系统地讲解了 13.56MHz 线圈天线的工作原理、设计方法、设计考量以及使用 HFSS 和 CST 仿真分析线圈天线的具体操作，同时还介绍了 13.56MHz 线圈天线匹配电路的设计和调试。通过该套课程的学习，可以帮助您快速学习掌握 13.56MHz 线圈天线及其匹配电路的原理、设计和调试…

详情浏览：http://www.edatop.com/peixun/antenna/116.html

---

### 我们的课程优势：

※ 成立于 2004 年，10 多年丰富的行业经验，

※ 一直致力并专注于微波射频和天线设计工程师的培养，更了解该行业对人才的要求

※ 经验丰富的一线资深工程师讲授，结合实际工程案例，直观、实用、易学

### 联系我们：

※ 易迪拓培训官网：http://www.edatop.com

※ 微波 EDA 网：http://www.mweda.com

※ 官方淘宝店：http://shop36920890.taobao.com